



Temperature Variation in a Homogeneous Sphere Induced by the Tide-Generating Force

JIANGCUN ZHOU,¹ ERNIAN PAN,² HEPING SUN,^{1,3} JIANQIAO XU,¹ and XIAODONG CHEN¹

Abstract—In this paper, we present a semi-coupled theory to compute the temperature variation due to the tide-generating force. The tidal volume strain is first derived in a pure elastic homogeneous sphere, in terms of the classic Love’s solution. Then the temperature variation is obtained by solving the inhomogeneous heat conduction equation by considering both the isothermal and adiabatic conditions on the surface. The results show that the magnitude of the tidal temperature variation can be more than 1 mK, which is detectable by the current precision thermometer.

Keywords: Tide-generating force, volume strain, temperature variation, heat conduction.

1. Introduction

It is well known that a solid medium will expand when it is heated and contract when cooled. This is due to the combined effects of the heat conduction in the medium and the related elastic deformation, i.e. expansion or compaction. Likewise, if a medium expands or contracts by an external force, the temperature will change accordingly.

With regard to the Earth, there are many studies on its deformation from different sources. A typical source origin is due to both the attraction from the Moon and the Sun, as well as from other planets, and the relative movements of these bodies, which is called the tide-generating force. It was Love (1911) who systematically investigated the Earth’s

deformation and derived the regular solution for a homogeneous Earth. This solution has been actively used in Earth science (e.g. Takagi & Okubo, 2017; Tang & Sun, 2017), including the tide phenomenon (e.g. Melchior, 1978), as tide affects the observations, for example, of displacement, gravity, tilt and strain, on and in the Earth.

Since significant deformation of the Earth occurs under the tide-generating force, there must be heat transport within it. As such, the temperature within the Earth will change. Actually, this temperature variation phenomenon was recently observed by the high-precision thermometer LogBox microT, whose resolution is 0.2 mK (10^{-3} K) (Jahr et al., 2020). Obvious tidal modulation was detected in the temperature recordings, which showed temperature variation up to a magnitude of milli-Kelvins. While a correlation between the temperature variation and the Earth’s tides has been observed (van Ruymbeke et al., 1991), no investigation has concentrated on the mechanism, i.e., how the Earth’s tide affects the temperature. This motivates the present study.

The coupling deformation and heat conduction problems are mostly studied in material and engineering sciences, which have small spatial scale (e.g., Vattre & Pan, 2021; Vattre et al., 2021), based on the theory of thermoelasticity (Biot, 1956). In Earth science, Fang et al. (2014) proposed a theory on surface heat loading for a homogeneous Earth. That model was advanced to a layered and anisotropic sphere (Zhou et al., 2021). However, these solutions cannot be applied to compute the temperature variation due to tides because the volume-change-induced temperature was neglected. Therefore, in this paper we propose a new theory to consider this effect. For simplicity, we start with a homogeneous sphere.

¹ State Key Laboratory of Geodesy and Earth’s Dynamics, Innovation Academy for Precision Measurement Science and Technology, Chinese Academy of Sciences, Wuhan 430077, China. E-mail: chenxd@whigg.ac.cn

² Disaster Prevention and Water Environment Research Center, National Yang Ming Chiao Tung University, 1001 University Rd., Hsinchu 300, Taiwan.

³ University of Chinese Academy of Sciences, Beijing 100049, China.

2. Theory

In this section, to simplify the problem, we apply a simple semi-coupled theory involving temperature and elastic deformation: namely, we consider the temperature variation due to tidal deformation while neglecting the deformation due to the tide-induced temperature variation, since the latter effect is of one order smaller. Furthermore, we use a uniform and isotropic Earth model to conserve the qualitative description of tidal temperature variation. In so doing, we can first compute the tidal deformation and then the temperature change.

2.1. Tidal Deformation

We consider the problem in the spherical coordinate system, as shown in Fig. 1. We denote the radius of the sphere by a , density by ρ , and Lamé's constants by λ and μ . The general solutions of the deformation induced by any internal or external force in a homogeneous, self-gravitating, compressible and isotropic sphere were derived by Love (1911). Therefore, the tidal deformation can be presented in terms of these three general solutions (e.g. Okubo, 1988).

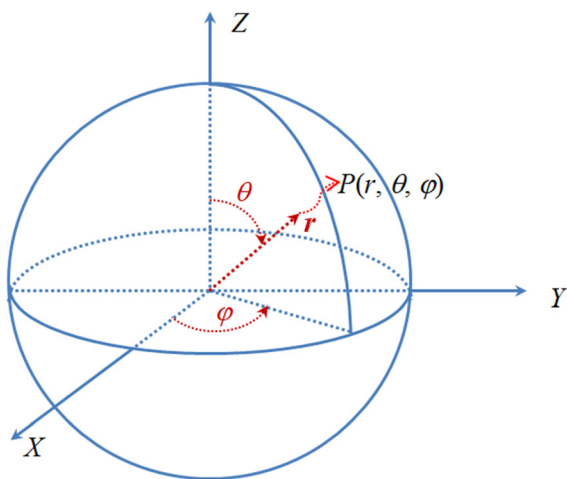


Figure 1

Sketch map of a spherical system [the location of a point P inside the sphere is denoted by (r, θ, φ)]

$$\begin{aligned} \mathbf{X}(r) &= [U_L, nU_M, n\Phi, rT_L/n, rT_M, rQ]^T \\ &= \begin{bmatrix} \mathbf{D}(r) \\ \mathbf{E}(r) \end{bmatrix} \mathbf{J}(r) \mathbf{c}, \quad 0 \leq r \leq a \end{aligned} \quad (1)$$

in which $U_L, U_M, \Phi, T_L, T_M, Q$ are respectively the spherical harmonic expansion coefficients of the vertical and horizontal displacements, additional potential, vertical normal stress, vertical shear stress, and gravity flux (see Pan et al., 2015), all the functions of the radial component r of the spherical coordinate system, and

$$[\mathbf{D}(r)] = \frac{1}{r} \begin{bmatrix} nh^+ - f^+ z_n(k^+ r) & nh^- - f^- z_n(k^- r) & n \\ nh^+ + nz_n(k^+ r) & nh^- + nz_n(k^- r) & n \\ 3\gamma n f^+ r & 3\gamma n f^- r & n^2 \gamma r \end{bmatrix}, \quad (2a)$$

$$[\mathbf{E}(r)] = \frac{1}{r} \begin{bmatrix} E_2^+/n & E_2^-/n & 2\mu(n-1) \\ E_4^+ & E_4^- & 2\mu(n-1) \\ E_6^+ r & E_6^- r & 2n(n-1)\gamma r \end{bmatrix}, \quad (2b)$$

$$[\mathbf{J}(r)] = \begin{bmatrix} j_n(k^+ r) & 0 & 0 \\ 0 & j_n(k^- r) & 0 \\ 0 & 0 & r^n \end{bmatrix} \quad (2c)$$

with

$$\begin{aligned} E_2^\pm &= -(\lambda + 2\mu)(k^\pm r)^2 f^\pm + 2\mu\{n(n-1)h^\pm \\ &\quad + [2f^\pm + n(n+1)]z_n(k^\pm r)\} \\ E_4^\pm &= \mu[(k^\pm r)^2 + 2(n-1)h^\pm - 2(f^\pm + 1)z_n(k^\pm r)] \\ E_6^\pm &= 3\gamma[(2n+1)f^\pm - nh^\pm], \end{aligned} \quad (3)$$

and

$$(k^\pm)^2 = \frac{2\gamma}{\alpha^2} \left(1 \pm \sqrt{1 + n(n+1) \frac{\alpha^2}{4\beta^2}} \right), \quad (4a)$$

$$\gamma = \frac{4\pi G\rho}{3}; \quad f^\pm = (k^\pm)^2 \frac{\beta^2}{\gamma}; \quad h^\pm = f^\pm - n - 1, \quad (4b)$$

$$z_n(x) = \frac{x j_{n+1}(x)}{j_n(x)} \quad (4c)$$

and \mathbf{c} is an unknown constant vector to be determined. In Eq. (4), α and β are respectively the P - and S -wave velocities which are related to Lamé's constants and mass density, and $j_n(x)$ is the spherical Bessel function of the first kind of order n .

The coefficient vector \mathbf{c} is determined from the following conditions on the surface (e.g. Sun & Dong, 2013)

$$\mathbf{T}_a = \begin{pmatrix} rT_L(r=a) \\ rT_M(r=a) \\ rQ(r=a) \end{pmatrix} = \begin{pmatrix} 0 \\ 0 \\ 2n+1 \end{pmatrix} \quad (5)$$

i.e.

$$\mathbf{c} \equiv \begin{pmatrix} C^+ \\ C^- \\ C \end{pmatrix} = [\mathbf{J}(a)]^{-1} [\mathbf{E}(a)]^{-1} \mathbf{T}_a \quad (6)$$

Finally, the tidal deformation of the entire sphere is determined by Eq. (1).

$$\mathbf{U}(r) = \begin{pmatrix} U_L \\ nU_M \\ n\Phi \end{pmatrix} = \mathbf{D}(r)\mathbf{J}(r)[\mathbf{J}(a)]^{-1}[\mathbf{E}(a)]^{-1}\mathbf{T}_a. \quad (7)$$

2.2. Temperature Variation in Frequency Domain

The temperature variation T , relative to the uniform reference temperature T_0 , satisfies the heat conduction equation (Biot, 1956),

$$\begin{aligned} \rho c_p \frac{\partial T}{\partial t} + B \left(\frac{\partial e_{\theta\theta}}{\partial t} + \frac{\partial e_{\phi\phi}}{\partial t} + \frac{\partial e_{rr}}{\partial t} \right) \\ T_0 - \kappa \left[\left(\frac{\partial^2 T}{\partial r^2} + \frac{2}{r} \frac{\partial T}{\partial r} \right) \right. \\ \left. + \frac{1}{r^2} \left(\frac{\partial^2 T}{\partial \theta^2} + \cot \theta \frac{\partial T}{\partial \theta} + \frac{\partial^2 T}{\sin^2 \theta \partial \phi^2} \right) \right] = 0, \end{aligned} \quad (8)$$

where c_p is the specific heat in J/(kg K), ρ is again the mass density in kg/m³, $B = (3\lambda + 2\mu)\alpha_c$, where α_c is the thermal expansion coefficient in K⁻¹, κ is the thermal conductivity in W/(m K), and t is the time in seconds. The dimensionless strains in the spherical coordinates are related to the displacement $\mathbf{u} = (u_r, u_\theta, u_\phi)$ as

$$\left. \begin{aligned} e_{rr} &= \frac{\partial u_r}{\partial r}; \quad e_{\theta\theta} = \frac{\partial u_\theta}{r \partial \theta} + \frac{u_r}{r} \\ e_{\phi\phi} &= \frac{\partial u_\phi}{r \sin \theta \partial \phi} + \frac{\cot \theta u_\theta}{r} + \frac{u_r}{r} \\ 2e_{\theta\phi} &= \frac{\partial u_\phi}{r \partial \theta} - \frac{\cot \theta u_\phi}{r} + \frac{\partial u_\theta}{r \sin \theta \partial \phi} \\ 2e_{r\theta} &= \frac{\partial u_\theta}{\partial r} + \frac{\partial u_r}{r \partial \theta} - \frac{u_\theta}{r} \\ 2e_{r\phi} &= \frac{\partial u_r}{r \sin \theta \partial \phi} + \frac{\partial u_\phi}{r \partial r} - \frac{u_\phi}{r} \end{aligned} \right\} \quad (9)$$

For tidal deformation, the static theory is commonly applied since the effect of the frequency is negligible. However, when the temperature, i.e. heat issue, is involved, the frequency effect is significant and, in general, cannot be neglected.

For a specific tidal constituent, the temperature change will depend on time in the form of $e^{i\omega t}$, with i being the imaginary number and ω the angular frequency. Therefore, we can apply the Fourier transform to Eq. (8) to arrive at

$$\begin{aligned} \frac{\partial^2 T}{\partial r^2} + \frac{2}{r} \frac{\partial T}{\partial r} + \frac{1}{r^2} \left(\frac{\partial^2 T}{\partial \theta^2} + \cot \theta \frac{\partial T}{\partial \theta} + \frac{\partial^2 T}{\sin^2 \theta \partial \phi^2} \right) \\ - \frac{i\omega \rho c_p}{\kappa} T \\ = \frac{i\omega B T_0}{\kappa} (e_{rr} + e_{\theta\theta} + e_{\phi\phi}) \end{aligned} \quad (10)$$

in which the transformed variables are denoted by the same symbols for conciseness.

We also apply the spherical harmonic expansion to the variables, which leads us to the following identity in terms of the spherical harmonic expansion coefficients of the temperature and elastic displacements

$$\begin{aligned} \frac{d^2 \tau}{dr^2} + \frac{2}{r} \frac{d\tau}{dr} + \left[-\frac{i\omega \rho c_p}{\kappa} - \frac{n(n+1)}{r^2} \right] \tau \\ = \frac{i\omega B T_0}{\kappa} \left[\frac{dU_L}{dr} + \frac{2U_L}{r} - \frac{n(n+1)U_M}{r} \right] \end{aligned} \quad (11)$$

in which τ is the expansion coefficient of the temperature T .

Substituting the tidal displacements obtained from Eqs. (1) to (6), we have, after some algebra,

$$\begin{aligned} \frac{d^2\tau}{dr^2} + \frac{2}{r} \frac{d\tau}{dr} + \left[-\frac{i\omega\rho c_p}{\kappa} - \frac{n(n+1)}{r^2} \right] \tau \\ = -\frac{i\omega BT_0}{\kappa} \left[C^\pm f^\pm(k^\pm)^2 j_n(k^\pm r) \right]. \end{aligned} \quad (12)$$

It should be noted that the inhomogeneous term has two components with superscripts + and -, i.e. the sum of both. We find that the third regular solution, determined by the coefficient C in Eq. (6), contributes nothing to the inhomogeneous part of Eq. (11). Thereafter, terms with the superscripts + and - mean summation of these two terms.

The general solution to Eq. (12) can be easily obtained because the solution is the spherical Bessel function. It should be noted that there is no heat source in the Earth's centre so the following condition should be satisfied:

$$\frac{d\tau(r=0)}{dr} = 0. \quad (13)$$

Thus, the spherical Bessel function of the second kind should be omitted from the general solution. Then the general solution is

$$\tau^g(r) = D j_n(pr) \quad (14)$$

in which the superscript g denotes the general solution, D is an unknown constant to be determined, j_n is the spherical Bessel function of the first kind of order n , and

$$p = \sqrt{-\frac{i\omega\rho c_p}{\kappa}}. \quad (15)$$

The particular solution can be derived as

$$\tau^p = \frac{i\omega BT_0 C^\pm f^\pm(k^\pm)^2}{\kappa(k^\pm)^2 + i\omega\rho c_p} j_n(k^\pm r). \quad (16)$$

We consider here two commonly used thermal conditions on the surface of the Earth, i.e. isothermal and adiabatic conditions.

2.2.1 Isothermal Case

In this case, the following boundary condition is satisfied

$$\tau(r=a) = 0. \quad (17)$$

Therefore, the unknown constant D is determined to be

$$D = -\frac{i\omega BT_0 C^\pm f^\pm(k^\pm)^2 j_n(k^\pm a)}{\kappa(k^\pm)^2 + i\omega\rho c_p j_n(pa)}. \quad (18)$$

Then, temperature variation is

$$\begin{aligned} \tau = \left[-\frac{i\omega BT_0 C^\pm f^\pm(k^\pm)^2 j_n(k^\pm a)}{\kappa(k^\pm)^2 + i\omega\rho c_p} \right] \frac{j_n(pr)}{j_n(pa)} \\ + \left[\frac{i\omega BT_0 C^\pm f^\pm(k^\pm)^2 j_n(k^\pm r)}{\kappa(k^\pm)^2 + i\omega\rho c_p} \right]. \end{aligned} \quad (19)$$

It should be noted that the brackets on the right-hand side in Eq. (19) have two terms.

2.2.2 Adiabatic Case

In this case, the following boundary condition is satisfied

$$\frac{d\tau(r=a)}{dr} = 0. \quad (20)$$

Then the unknown constant is

$$D = -\frac{i\omega BT_0 C^\pm f^\pm(k^\pm)^2 j_n'(k^\pm a)}{\kappa(k^\pm)^2 + i\omega\rho c_p j_n'(pa)}. \quad (21)$$

Consequently, the final solution is

$$\begin{aligned} \tau = \left[-\frac{i\omega BT_0 C^\pm f^\pm(k^\pm)^2 j_n'(k^\pm a)}{\kappa(k^\pm)^2 + i\omega\rho c_p} \right] \frac{j_n(pr)}{j_n'(pa)} \\ + \left[\frac{i\omega BT_0 C^\pm f^\pm(k^\pm)^2 j_n(k^\pm r)}{\kappa(k^\pm)^2 + i\omega\rho c_p} \right] \end{aligned} \quad (22)$$

in which the prime means derivative with respect to r . Again, two terms in the brackets on the right-hand side of Eq. (22) should be noted. Also note that the coefficients C^+ and C^- are given by Eq. (6).

2.3. Temperature Variation in Time Domain

The boundary condition in Eq. (5) implies that the deformation is a response to the unit tide-generating potential. Therefore, the temperature variation for one tidal constituent is the product of τ derived in Sect. 2.2 and the tide-generating potential of this constituent. The latter is expressed by

$$V_{\omega}(r, \theta, \lambda, t) = A_{\omega} G_{nm}(r, \theta) \begin{cases} \cos(\omega t + \chi_0) \\ \sin(\omega t + \chi_0) \end{cases} \quad (23)$$

in which A_{ω} is the frequency-dependent relative coefficient of each constituent, which can be obtained from the potential table (e.g. Xi, 1989), and G_{nm} (n and m are respectively the harmonic degree and order) represents the geodetic coefficient which can be written as

$$\left. \begin{aligned} G_{20} &= \frac{1}{2} D_2 \left(\frac{r}{R}\right)^2 (1 - 3 \cos^2 \theta) \\ G_{21} &= D_2 \left(\frac{r}{R}\right)^2 \sin 2\theta \\ G_{22} &= \frac{D_2}{2} \left(\frac{r}{R}\right)^2 \sin^2 \theta \end{aligned} \right\} \quad (24a)$$

for degree 2, in which D_2 is the degree 2 Doodson number for the Moon,

$$\left. \begin{aligned} G_{30} &= \frac{\sqrt{5}}{2} D_2 \left(\frac{r}{R}\right)^3 \cos \theta (3 - 5 \cos^2 \theta) \\ G_{31} &= \frac{3\sqrt{15}}{16} D_2 \left(\frac{r}{R}\right)^2 \sin \theta (1 - 5 \cos^2 \theta) \\ G_{32} &= \frac{3\sqrt{3}}{2} D_2 \left(\frac{r}{R}\right)^2 \cos \theta \sin^2 \theta \\ G_{33} &= D_2 \left(\frac{r}{R}\right)^2 \sin^3 \theta \end{aligned} \right\} \quad (24b)$$

for degree 3, and

$$\left. \begin{aligned} G_{40} &= \frac{1}{8} D_2 \left(\frac{r}{R}\right)^4 (3 - 30 \cos^2 \theta + 35 \cos^4 \theta) \\ G_{41} &= \frac{224}{(13 + \sqrt{393})\sqrt{390 + 2\sqrt{393}}} D_2 \left(\frac{r}{R}\right)^4 \sin 2\theta (3 - 7 \cos^2 \theta) \\ G_{42} &= \frac{7}{9} D_2 \left(\frac{r}{R}\right)^4 \sin^2 \theta (1 - 7 \cos^2 \theta) \\ G_{43} &= \frac{16}{3\sqrt{3}} D_2 \left(\frac{r}{R}\right)^4 \cos \theta \sin^3 \theta \\ G_{44} &= D_2 \left(\frac{r}{R}\right)^4 \sin^4 \theta \end{aligned} \right\} \quad (24c)$$

for degree 4. Notice that χ_0 is the initial astronomical argument, which is in terms of the Doodson code and longitude of interest. The selection of cosine or sine function depends on the potential table, as in Xi (1989).

The temperature variation due to a unit tidal potential in the frequency domain is a complex number, and can be represented by

$$\tau(\omega) = |\tau(\omega)| e^{iq} \quad (25)$$

in which $|\tau(\omega)|$ means absolute value of $\tau(\omega)$, and q is the principle argument of complex $\tau(\omega)$. This means that the temperature variation precedes the tidal deformation by q in the phase.

Therefore, by multiplying $\tau(\omega)$ by the tidal potential, the tidal temperature variation is represented by

$$T(r, \theta, \varphi, t) = \sum_{\omega} |\tau(\omega)| A_{\omega} G_{nm}(r, \theta) \begin{cases} \cos(\omega t + \chi_0 + q) \\ \sin(\omega t + \chi_0 + q) \end{cases} \quad (26)$$

3. Results and Discussion

In this section, we set the parameters of the homogeneous sphere as follows. The density is set as 5517 kg/m^3 , Lamé's constants are $\lambda = 3.5288 \times 10^{11} \text{ N/m}^2$, and $\mu = 1.4519 \times 10^{11} \text{ N/m}^2$ according to Wu and Peltier (1982), which are the averaged values of the Earth. The thermal parameters are set as $T_0 = 300 \text{ K}$, $C_p = 500 \text{ J/(kg K)}$, $\kappa = 10 \text{ W/(m K)}$, $\alpha_c = 1.0 \times 10^{-5} \text{ K}^{-1}$. To compare with the observation in Jahr et al. (2020), i.e. their fig. 3, we also compute the temperature variation at Göttingen University (the location is about $\theta = 51.541^\circ$, $\varphi = 9.936^\circ$) in the same time band.

Figure 2a shows the temperature change. It is observed that the magnitude is smaller than 0.1 mK , which is below the accuracy of the thermometer. Moreover, we find that the results for isothermal and adiabatic cases are nearly the same. This is because the general solution contributes almost nothing to the final result, and it is the particular solution that dominates the result. Because the particular solutions of the two cases are the same, the results of the two cases are also the same.

Since the temperature variation is directly due to the volume strain, here for comparison, we also show the volume strain at 60 m depth in Fig. 1b. The temperature variation and volume strain are almost anti-phase. This can be derived from the particular solutions in Eq. (16). In the denominator, there are two terms: The first term is negligible compared to the second, according to the values of the parameters.

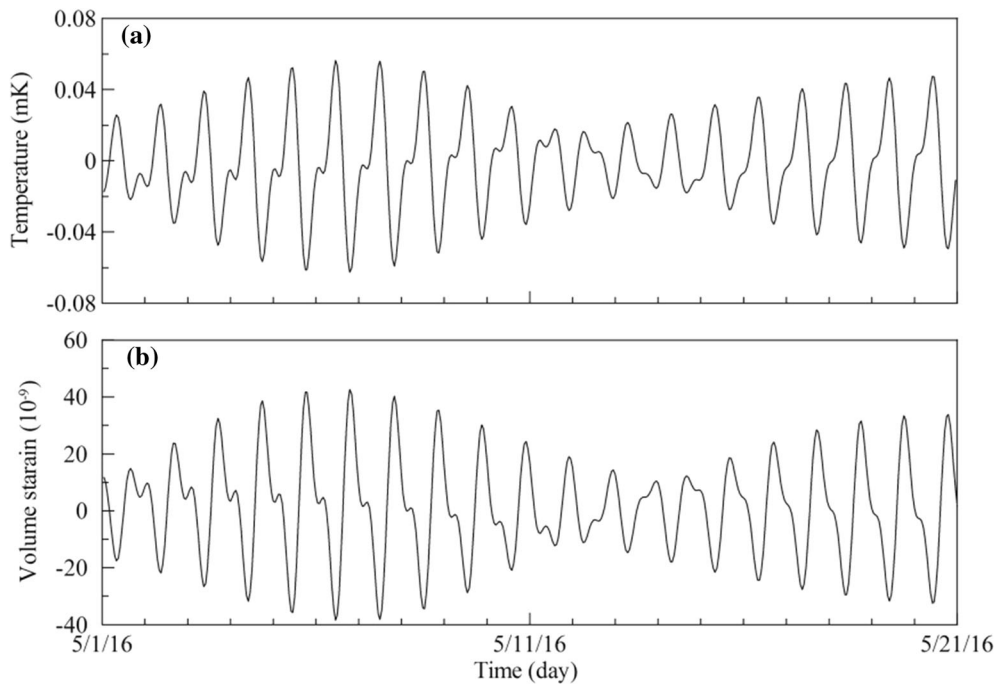


Figure 2
Temperature variation and volume strain at 60 m depth due to the tide-generating force

This means that the temperature variation is exactly $BT_0/\rho C_p$ times that of the volume strain but has an opposite sign. This also shows that the choice of the thermal conductivity value will not affect the results.

One may argue that the computed temperature is so small compared to the observed one that the observed temperature variation (about 1–2 mK) is not

due to the tide-generating force. However, one should keep in mind the following facts:

- (1) First, a homogeneous sphere is used. The Love numbers on the surface computed from this model are $h_2 = 0.5223$ and $l_2 = 0.1424$, respectively. For the realistic PREM model (Dziewonski & Anderson, 1981), they are about 0.6 and 0.3, respectively. Therefore, the

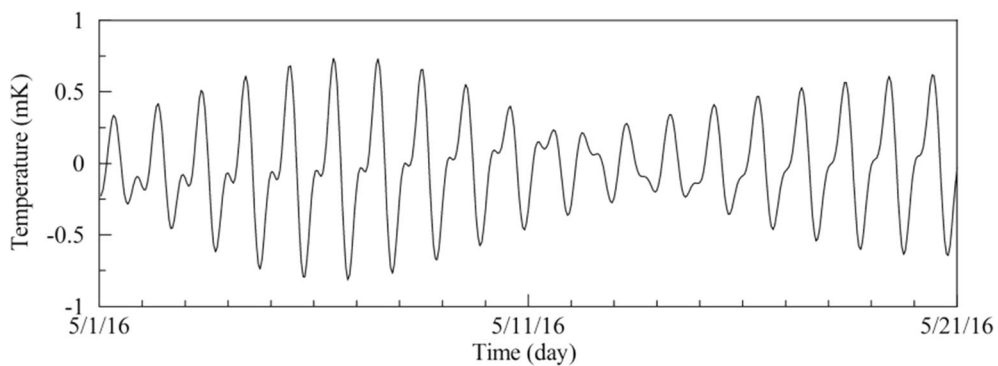


Figure 3
Similar to Fig. 2a, but in terms of realistic thermal parameters

computed volume strain will be smaller than that in the more realistic Earth, so does the temperature variation.

- (2) Second, we used the averaged density of the Earth, 5517 kg/m^3 , in the heat conduction equation. However, near the surface the density is smaller, around 2600 kg/m^3 in the PREM model (Dziewonski & Anderson, 1981). This also makes the temperature variation smaller.
- (3) Finally, we used the thermal parameters of rock. However, the soil in the ground of the observatory contains clay and silt besides claystone, sandstone, maristone, etc. (Jahr et al., 2020). Meanwhile, the soil is porous, containing water in general. The thermal expansion coefficients of clay and water are both larger than that of rock, $1 \times 10^{-5} \text{ K}^{-1}$, as we set. It is $3.4 \times 10^{-5} \text{ K}^{-1}$ for clay (McTigue, 1986) and $27 \times 10^{-5} \text{ K}^{-1}$ for water (Delage, 2013).

In the following new example, we set the porosity at 10% and weight the thermal expansion coefficients of clay and water, which gives us a weighted value of $5.76 \times 10^{-5} \text{ K}^{-1}$. Similarly, we obtained the weighted density at 2440 kg/m^3 . In terms of these updated parameters, the new temperature variation is shown in Fig. 3.

From Fig. 3, we find that the amplitude of the temperature variation is about 1 mK, which is now comparable to that observed by Jahr et al. (2020). The volume strain is the same as that shown in Fig. 2b, since we still use the averaged parameters of the Earth, as the model parameters in the uppermost layer do not affect the low-degree Love numbers. Again, the temperature and volume strain are in opposite phase.

It should be noted that the volume strain computed based on a homogeneous sphere will differ from that based on a realistic Earth model, such as the PREM. This may be why our volume strain is not exactly the same as that in Jahr et al. (2020). Furthermore, although we take the porous medium into account in setting the thermal parameters, the fluid is not coupled in the boundary-value problem. It is well known that the tide-generating force causes underground fluid flow. The typical phenomenon is tidal well level change. Even a low flow rate transfers

more heat than the rock does. Hence, the flow in the porous earth due to the tide-generating force will induce temperature variation, and it should be considered in the future.

4. Conclusions

We have proposed a simple approach to evaluate the tidal temperature variation by considering the deformation-induced temperature change while neglecting the resulting temperature-induced deformation. This treatment causes one-order smaller magnitude uncertainty in the result.

The numerical results show that the temperature variation caused by the tide-generating force is detectable at the locations where the thermal parameters are specific. The magnitude of the tidal temperature variation can be up to 1 mK under both isothermal and adiabatic boundary conditions. Our results show that the volume strain, i.e. the inhomogeneous part in the heat conduction equation, dominates the final results. This is why the results under the two boundary conditions are nearly the same.

Fluid flow may cause significant temperature variation. Therefore, the fluid-coupled thermoelastic deformation theory is required to obtain a more accurate solution, which will be investigated in future work.

Funding

This study was financially supported by the National Key R&D Program of China (2021YFA0715100), the Chinese Academy of Sciences (Grant no. XDB41000000), the National Natural Science Foundation of China projects (Grant nos. 41874026, 41874094 and 42174101) (JZ, JX, XC), and the NYCU Chair Professorship (EP).

Declarations

Conflict of interest The authors declare that they have no conflict of interest.

Open Access This article is licensed under a Creative Commons Attribution 4.0 International License, which permits use, sharing, adaptation, distribution and reproduction in any medium or format, as long as you give appropriate credit to the original author(s) and the source, provide a link to the Creative Commons licence, and indicate if changes were made. The images or other third party material in this article are included in the article's Creative Commons licence, unless indicated otherwise in a credit line to the material. If material is not included in the article's Creative Commons licence and your intended use is not permitted by statutory regulation or exceeds the permitted use, you will need to obtain permission directly from the copyright holder. To view a copy of this licence, visit <http://creativecommons.org/licenses/by/4.0/>.

Publisher's Note Springer Nature remains neutral with regard to jurisdictional claims in published maps and institutional affiliations.

REFERENCES

- Biot, M. A. (1956). Thermoelasticity and irreversible thermodynamics. *Journal of Applied Physics*, 27, 240–253.
- Delage, P. (2013). On the thermal impact on the excavation damaged zone around deep radioactive waste disposal. *Journal of Rock Mechanics and Geotechnical Engineering*, 5, 179–190.
- Dziewonski, A. M., & Anderson, D. L. (1981). Preliminary reference Earth model. *Physics of the Earth and Planetary Interiors*, 25, 297–356.
- Fang, M., Dong, D., & Hager, B. H. (2014). Displacements due to surface temperature variation on a uniform elastic sphere with its centre of mass stationary. *Geophysical Journal International*, 196, 194–203.
- Love, A. E. H. (1911). *Some problems of geodynamics*. Cambridge University Press.
- Jahr, T., Buntebarth, G., & Sauter, M. (2020). Earth tides as revealed by micro-temperature measurements in the subsurface. *Journal of Geodynamics*, 136, 101718.
- McTigue, D. F. (1986). Thermoelastic response of fluid-saturated porous rock. *Journal of Geophysical Research*, 91, 9533–9542.
- Melchior, P. (1978). *The tides of the planet Earth* (p. 609). Pergamon.
- Okubo, S. (1988). Asymptotic solutions to the static deformation of the Earth-I. Spheroidal mode. *Geophysical Journal International*, 92, 39–51.
- Pan, E., Chen, J. Y., Bevis, M., Bordoni, A., Barletta, V. R., & Molavi Tabrizi, A. (2015). An analytical solution for the elastic response to surface loads imposed on a layered, transversely isotropic, and self-gravitating Earth. *Geophysical Journal International*, 203, 2150–2181.
- Sun, W., & Dong, J. (2013). Relation of dislocation Love numbers and conventional Love numbers and corresponding Green's functions for a surface rupture in a spherical earth model. *Geophysical Journal International*, 193, 717–733.
- Takagi, Y., & Okubo, S. (2017). Internal deformation caused by a point dislocation in a uniform elastic sphere. *Geophysical Journal International*, 208, 973–991.
- Tang, H., & Sun, W. (2017). Asymptotic expressions for changes in the surface coseismic strain on a homogeneous sphere. *Geophysical Journal International*, 209, 202–225.
- van Ruymbeke, M., Westerhaus, M., & Fernandez, J. (1991). Temperature measurements. In E. Helsinki (Ed.) *Schweizerbart'sche Verlagsbuchhandlung Stuttgart*. Proceedings of 11th international symposium on earth tides 1989 (pp. 73–83)
- Vatire, A., & Pan, E. (2021). Thermoelasticity of multilayered plates with imperfect interfaces. *International Journal of Engineering Sciences*, 158, 103409.
- Vatire, A., Pan, E., & Chiaruttini, V. (2021). Free vibration of fully coupled thermoelastic multilayered composites with imperfect interfaces. *Composite Structures*, 259, 113203.
- Wu, P., & Peltier, W. R. (1982). Viscous gravitational relaxation. *Geophysical Journal International*, 70, 435–485.
- Xi, Q. W. (1989). The precision of the development of tidal generating potential and some explanatory notes. *Bull Inf Marées Terrestres*, 105, 7396–7404.
- Zhou, J., Pan, E., & Bevis, M. (2021). Deformation due to surface temperature variation on a spherically layered, transversely isotropic and self-gravitating Earth. *Geophysical Journal International*, 225, 1672–1688.

(Received February 22, 2022, revised May 13, 2022, accepted May 29, 2022, Published online June 22, 2022)